Heliyon 10 (2024) e31254

Contents lists available at ScienceDirect

Heliyon

journal homepage: www.cell.com/heliyon

Research article

A comprehensive study about functionalization and de-functionalization of MOF-808 as a defect-engineered Zr-MOFs for selective catalytic oxidation

Negin Khosroshahi, Samira Doaee, Vahid Safarifard *, Sadegh Rostamnia **

Department of Chemistry, Iran University of Science and Technology, Tehran, 16846-13114, Iran

ARTICLE INFO

Keywords:
Methyl(phenyl)sulfide
Heterogeneous catalysis
Zr-MOF-808
Sulfide conversion

ABSTRACT

In metal–organic frameworks (MOFs), confined space as a chemical nanoreactor is as essential as coordinatively unsaturated metal site catalysis. The properties of MOFs can be adjusted through the incorporation of functional groups and open metal sites in frameworks that can modify the catalytic performance. In this regard, a set of defect-engineered MOFs, Ex-MOF-808(NH_2, NO_2, H) and Mix-MOF-808(NH_2, NO_2, H), were synthesized by ultrasonic-assisted linker exchange approach (Ex-MOFs) and solvothermal mixing ligand method (Mix-MOFs), respectively. Further, the relationship between the preparation method, structural properties, and catalytic efficiency of the prepared materials in the selective oxidation of methyl phenyl sulfide (MPS) has been investigated. By analyzing zeta potential, it was found that in the exchange method, the amount of defect and functional groups on the surface of MOFs are more than in the mixing method, which also affects the catalytic activity. In our contribution, mix-MOF-808(NO_2) carrying nitro groups at their organic linkers, which has a well-dispersion of nitro groups at the framework exhibits selective conversion of MPS to sulfone (91 %). Furthermore, the performance of stable heterogeneous catalysts was investigated for three cycles, which demonstrated their great potential for advanced catalytic oxidation.

1. Introduction

Recently, MOFs have received more and more attention due to their potential applications from researchers [1–3]. MOFs can be widely used as catalysts in the oxidation of sulfide due to their unique advantages (including a high surface area, high porosity, abundant active Lewis/Brønsted acidic or basic sites, and controllable pore size) [4–6]. Despite the many benefits of MOFs, these compounds have poor structural stability. The zirconium-based metal-organic framework (Zr-MOFs) not only has high stability and excellent catalytic performance, but also can be modified by organic ligands, topology design, and post-synthesis modification [7,8]. For Lewis acid-catalyzed reactions it was shown that trimesic acid defects are responsible for the catalytic activity of the Zr-MOF material [9,10]. Moreover, functionalization of the 1,3,5-benzenetricarboxylate linker allows obtaining of a family of isoreticular MOF-808 structures. Many kinds of research indicate the catalytic activity of Zr-MOFs with several functional groups. For example, UiO-66-NH_2 acts as a bifunctional catalyst with Lewis acid Zr-sites and Brønsted base –NH_2 sites, rendering it more active and selective

* Corresponding author.
** Corresponding author.
E-mail addresses: vsafarifard@iust.ac.ir (V. Safarifard), rostamnia@iust.ac.ir (S. Rostamnia).

https://doi.org/10.1016/j.heliyon.2024.e31254
Received 10 January 2024; Received in revised form 7 May 2024; Accepted 13 May 2024
Available online 14 May 2024

in catalytic reactions [11].

MOFs can be easily modified with some functional groups by using various functionalized ligands or through various methods [12–14]. Several strategies are integrating multiple ligands with identical linking chemistry to represent an efficient route to access multivariate MOFs with increased complexity and functions, such as a mixed linker, and post-synthetic linker exchange (PSE) methods [15]. In the realm of metal-organic frameworks, post-synthetic linker exchange and solvent-assisted linker exchange (SALE) represent two key strategies for the modification and functionalization of MOFs after their synthesis. PSE involves the replacement of original organic linkers within a pre-synthesized MOF with new ligands containing desired functionalities, achieved through immersion in a solution containing the new ligands [16]. This method offers precise control over functional group incorporation and has been advanced notably by Cohen's pioneering work, facilitating tailored properties for specific applications [17,18]. Conversely, SALE entails the exchange of original linkers with new ones in the presence of a coordinating solvent, offering simplicity and scalability. Farha's research has extensively explored SALE methods, demonstrating their utility in introducing functionalities and enhancing MOF properties for various applications [19,20]. Both strategies contribute significantly to MOF research, enabling the customization of MOF properties to meet diverse application requirements.

In the mixed-linker method, a series of MOFs is constructed through the incorporation of a second linker with a homogenous distribution of functional groups and open metal sites in the hole framework [21]. While post-synthetic modification is more common than the mixed linker method due to the lack of topological change, better and more control over the types of functional groups that can be included in the framework, and the lack of change in the main structure of the composition [22,23]. Moreover, in this method, the distribution of active sites at the surface of the framework is more than the mixed-linker method.

Organosulfur compounds, like sulfoxides and sulfones, are useful synthetic intermediates in organic chemistry for constructing various chemically and biologically active molecules, especially drugs, and natural products [24–26]. So, these sulfoxides and sulfones demonstrate varied applications such as anti-bacterial, anti-atherosclerotic, anti-fungal, etc. [27,28]. Among the array of methods utilized to synthesize sulfoxides or sulfones, sulfide oxidation is the most favorable one. During the oxidation process, sulfur compounds can be converted into sulfoxide or sulfone products by using effective catalysts and suitable oxidizing agents (such as molecular oxygen, hydrogen peroxide, and organic peroxides) and in mild operating conditions (at temperatures below 100 °C and ambient temperature) [29,30]. In this regard, different catalytic systems of organocatalysts, metal catalysts, enzymes, and organic–inorganic hybrid solid materials have been utilized for sulfide oxidation with H_2O_2 as an oxygen source. Organic transformations using conventional catalysts are possible, but there are several disadvantages, such as over-oxidation and toxic wastes [31]. First, they dissolve easily in polar solvents, which shortens their life, as a result, they are not suitable for large scale. Second, their specific surface area is low and limits exposure to catalytically active sites [32]. A more appropriate catalyst should be used to avoid these limitations. Among the various catalysts, metal-organic frameworks (MOFs) can be mentioned as efficient catalysts. MOF ligands with functional moieties such as amino groups aligned on their pore walls can act as active sites, which can increase their affinity in catalytic reactions via supramolecular interactions [33,34].

In this work, to investigate defect-engineered MOF catalysts, a set of the mixed-ligand Zr-MOF-808 family with specific ratios of trimesic acid and second linker (5-amino isophthalic acid, or 5-nitro isophthalic acid, or isophthalic acid linkers) were prepared by mixing ligand and ultrasonic-assisted exchanged-ligand strategies (named Ex-MOF). In this comprehensive study, the NH_2-functionalized linker was utilized as Brønsted base sites, while NO_2-isoBDC and isophthalic acid linkers were used for creating more Lewis acid sites. The prepared catalysts named Ex-MOF-808(NH_2, NO_2, H) and Mix-MOF-808(NH_2, NO_2, H), containing defect-inducing linkers, used in methyl(phenyl)sulfide oxidation with hydrogen peroxide under different reaction conditions. The results indicate that creating functional groups and open metal sites in frameworks leads to modifying the catalytic performance. In this regard, the catalytic activity of mix-MOF-808(NO_2) is higher than that of isoreticular mix-MOF-808-X (X: NH_2, H). Importantly, it was also demonstrated that the H_2O_2-based oxidation catalysis over mix-MOF-808(NO_2) has a genuinely heterogeneous nature.

2. Experimental section

2.1. Chemicals

All the reagents were analytical grade and were used without further purification. Zirconium tetrachloride ($ZrCl_4$, 98 %, Sigma-Aldrich), 1,3,5-benzene tricarboxylic acid (BTC, 98 %), 5-amino isophthalic acid (NH_2-isoBDC, 98 %), isophthalic acid (99 %, Sigma-Aldrich), 5-nitro-isophthalic acid (NO_2-isoBDC, 98 % Sigma-Aldrich), methyl(phenyl)sulfide (99 %, Sigma-Aldrich), acetonitrile, glacial acetic acid (CH_3COOH), trichloromethane ($CHCl_3$), N, N-dimethylformamide (DMF, C_3H_7NO,99.5 %), ethanol (CH_4O, 99.7 %), hydrogen peroxide (35 %, Sigma-Aldrich), acetone and other necessary chemicals were procured and used without further purification.

2.2. Measurement

The infrared spectra were recorded on a Nicolet Fourier Transform IR, Nicolet 100 spectrometer in the range 500–4000 cm^{-1} using the KBr disk technique. X-ray powder diffraction (XRD) measurements were performed using a Philips X'pert diffractometer with monochromated Cu-kα radiation ($\lambda = 1.54056$ Å). The simulated XRD powder pattern based on single crystal data was prepared using Mercury software. The used sonicator was a Samkoon Sonicator with adjustable power output (maximum 400 W at 20 kHz). The samples were characterized by a scanning electron microscope (SEM) (Philips XL 30 and S-4160) with gold coating. Surface area and pore size distribution were determined using the BET multilayer nitrogen adsorption method in a conventional volumetric technique

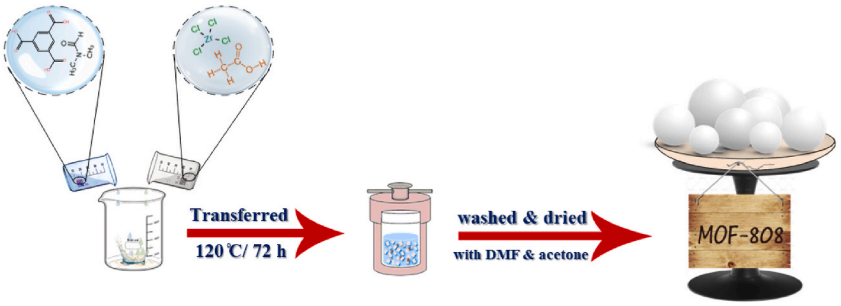

Fig. 1. Schematic diagram of the preparation process of Zr-MOF-808.

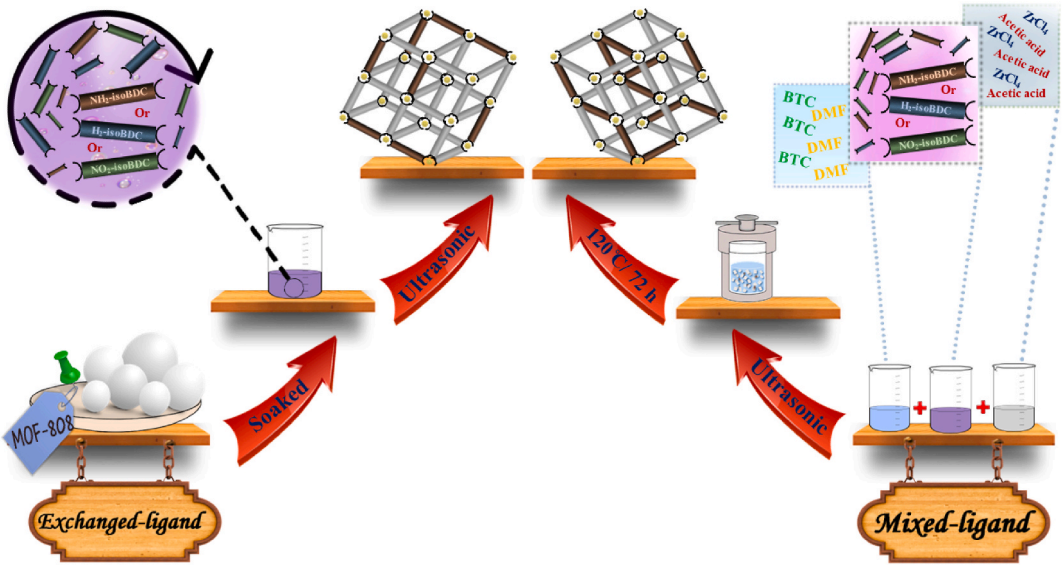

Fig. 2. Schematic diagram of the preparation process of MOF-808 (NH_2, NO_2, H) with two synthesis methods.

with a Micromeritics ASAP 2020 instrument. UV–visible DRS spectra were obtained with a Shimadzu MPC-2200 spectrophotometer. A Netzsch Thermoanalyzer STA 504 was used for the thermogravimetric analysis (TGA) with a heating rate of 10 °C/min under air atmosphere. Primary results for reaction progress were obtained by Gas Chromatography (GC) (Yonglin 6100; BP-5; 30 m × 0.25 × mm × 0.25 μm) with toluene as a general solvent for injection and nitrogen as an inert carrier gas. All yields referred to isolated products. The zeta potential was measured by the Horiba SZ100 instrument.

2.3. Synthesis and characterization of MOFs

2.3.1. Synthesis of MOF-808

The synthesis of the pure MOF-808 was accomplished following published synthesis procedures [35]. Generally, in a beaker $ZrCl_4$ (1.05 g, 4.5 mmol) was dissolved in a 45 mL glacial acetic acid solution. On the other hand, in the second beaker, H_3BTC (0.31 g, 1.5 mmol) was dissolved in 45 mL DMF. After both beakers are sonicating for 30 min, their contents are mixed. The mixture ($ZrCl_4$ and H_3BTC solutions), was put in an ultrasonic bath for 45 min. Later, the solution was transferred to a stainless-steel autoclave and then placed in an oven at 120 °C for 72 h. White precipitates formed after cooling to room temperature, which was separated by centrifugation. The resulting product was washed four times with DMF and acetone and put in the oven at 100 °C for 12 h, and then activation was performed in $CHCl_3$ at 50 °C for three days. Ultimately, the MOF-808 sample was dried in a vacuum for 24 h at 120 °C (Fig. 1).

2.3.2. Exchanged-ligand method for the synthesis of MOF-808(NH_2, NO_2, H)

According to the procedure mentioned above, 0.125 mmol (0.1711 g) MOF-808 was soaked in a solution containing 0.250 mmol 5-amino isophthalic acid (NH_2-isoBDC) in 5 mL DMF, under ultrasonic irradiation for 2 h. Rise to the next level, the resulting precipitate was separated by centrifugation and washed three times with DMF and ethanol, and dried at 100 °C under a vacuum. The synthesized MOF through ligand exchange method named Ex-MOF-808(NH_2). The previous process was repeated with isophthalic acid (H_2-

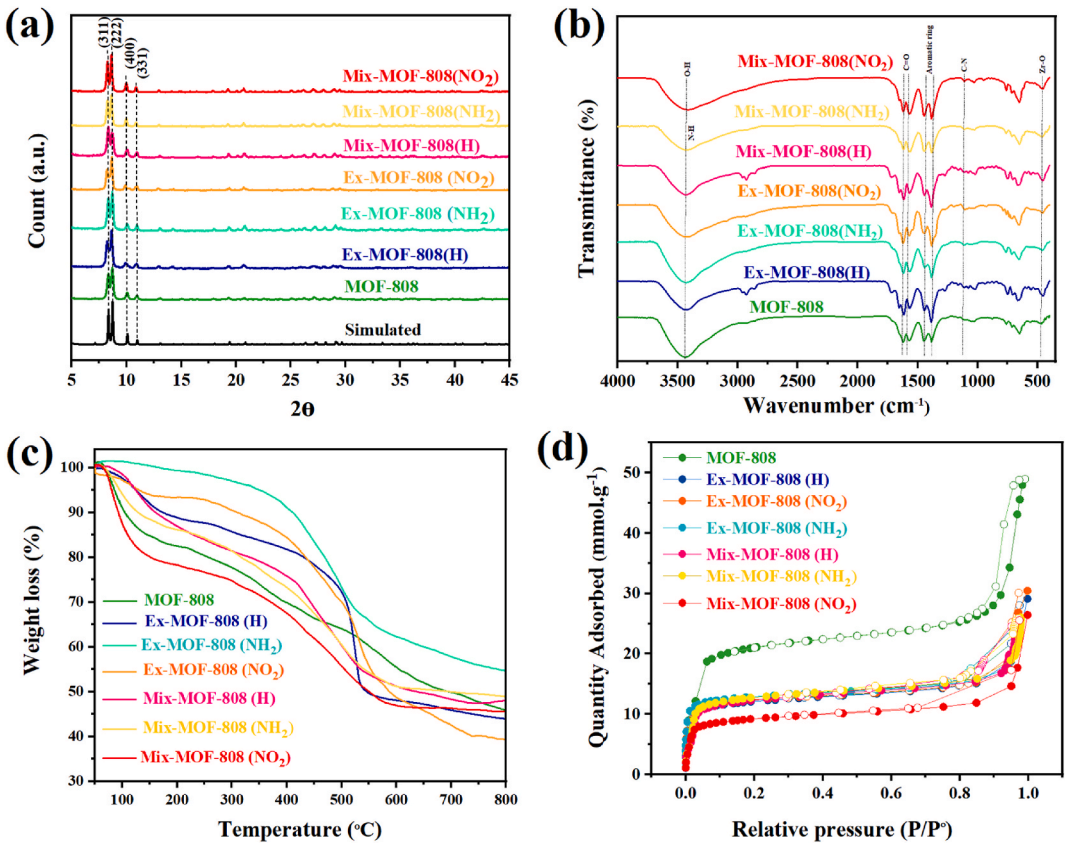

Fig. 3. a) Powder XRD pattern, (b) FT-IR spectra, (c) TGA plot, and (d) N_2 adsorption-desorption isotherms of all synthesized catalysts.

isoBDC) and 5-nitro-isophthalic acid (NO_2-isoBDC) ligands to synthesize the Ex-MOF-808(H), and Ex-MOF-808(NO_2) respectively (Fig. 2). The prepared compounds were characterized using various characterization methods.

2.3.3. Mixed-ligand synthesis of MOF-808 (NH_2, NO_2, H)

The procedure for mixed-ligand of MOF-808(X) synthesis has been reported previously [10]. Mix-MOF-808(X: NH_2, NO_2, H) materials were prepared by replacing 10 mol% of H_3BTC with equimolar amounts of defective linker: a) 5-aminoisophthalic acid (0.015 mmol) for Mix-MOF-808(NH_2) b) 5-nitroisophthalic acid (0.015 mmol) for Mix-MOF-808(NO_2) and c) Isophthalic acid (0.015 mmol) for Mix-MOF-808(H). The remaining synthesis steps were kept the same as for the MOF-808 material (Fig. 2).

2.4. General procedure for the oxidation experiments using MOF-808 derivatives

A 2 mL vial was charged with 0.1 mmol of methyl phenyl sulfide followed by the addition of acetonitrile. A catalyst of 0.01 mmol was then added to the mixture, and immediately after, hydrogen peroxide was introduced. The solution was stirred and allowed to react for a pre-determined period under ambient conditions. After the elapsed time, the sample was filtered to remove any impurities. The resulting product was subsequently analyzed using gas chromatography-mass spectrometry (GC-MS) (see electronic supporting information). The data obtained from these analyses allowed for the identification and characterization of the product, as well as the determination of its purity and yield. Finally, at the end of each reaction, the respective solid catalysts were isolated by centrifugation, washed carefully with acetonitrile and EtOH, and reused in the next catalytic cycle under identical reaction conditions.

3. Results and discussion

3.1. Characterization

3.1.1. Powder X-ray diffraction

Powder X-ray diffraction (PXRD) analysis was used to confirm the crystal structure of MOF-808 and its derivatives, and the results are shown in Fig. 3a. According to the depicted PXRD diagram, four sharp peaks can be seen at $2\Theta = 8.2°$, $8.6°$, $9.9°$, and $10.8°$, which are on planes 311, 222, 400, and 331, respectively [36,37]. On the other hand, by analyzing this graph, we realize that the crystallinity

Table 1
Specific surface areas, pore volume, and isotherm type of MOF-808-based catalysts.

Structure	Surface area (m^2/g)	Total pore volume (cm^3/g)	Isotherm type
MOF-808	1632.5	1.495	Type IV
Ex-MOF-808(H)	995.6	0.948	Type IV
Ex-MOF-808(NH_2)	1025.4	1.02	Type IV
Ex-MOF-808(NO_2)	1057.6	0.846	Type IV
Mix-MOF-808(H)	990.5	0.857	Type IV
Mix-MOF-808(NH_2)	1033	0.901	Type IV
Mix-MOF-808(NO_2)	859	0.839	Type IV

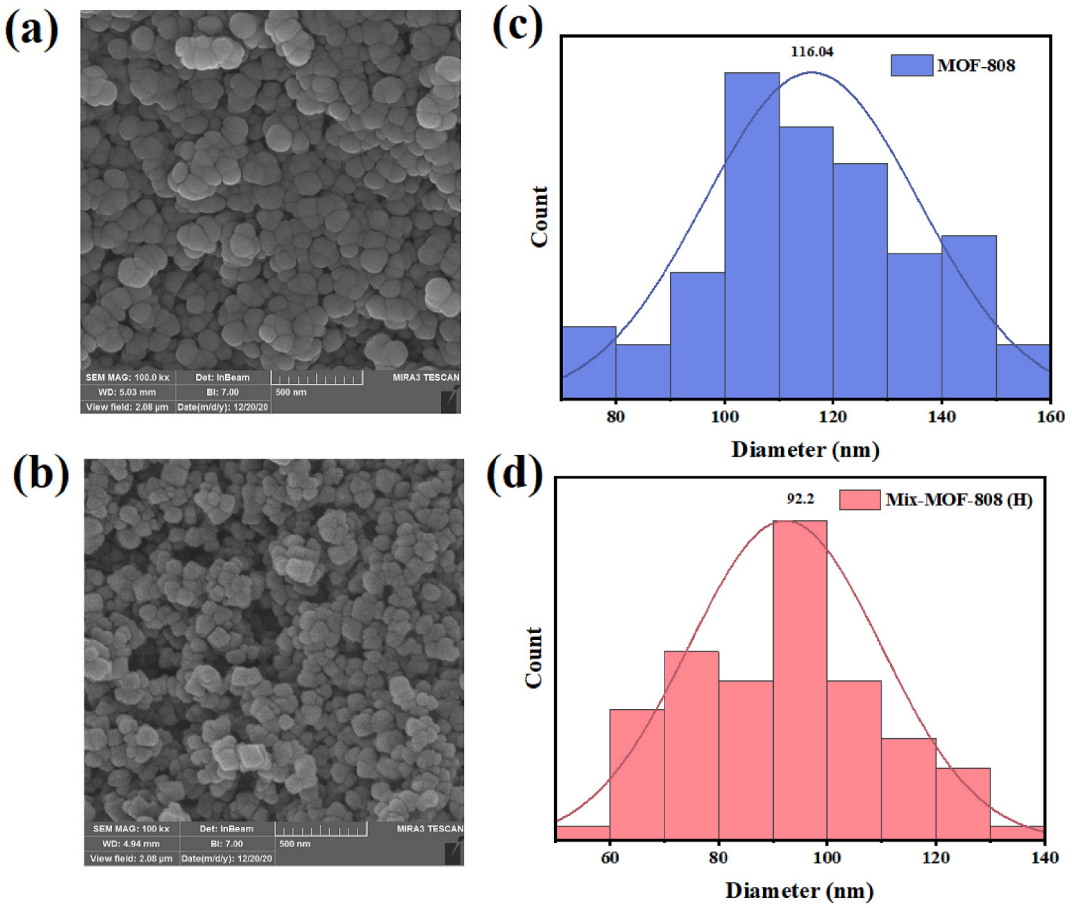

Fig. 4. FE-SEM images of samples (a) MOF-808, and (b) Mix-MOF-808(H). Particle size distribution of (c) MOF-808, and (d) Mix-MOF-808(H) according to FE-SEM images.

and structure of all the compounds are well compatible with the MOF-808 pattern. It is worth noting that all functionalized compounds have X-ray diffraction patterns similar to MOF-808 materials reported in the literature and simulated single crystals (space group Fd-3m, spn topology) [38].

The crystallite diameter (Dc) of samples obtained using the Debey-Scherrer equation:

$$D = K\lambda/\beta\cos\theta$$

Where β is the breadth of the observed diffraction line at its half intensity maximum, K is the so-called shape factor, which adequately carries a value of about 0.9, and λ is the wavelength of the X-ray source used in XRD. Calculated crystalline domain sizes are 51.5, 51.5, 45.6, 49.8, 61.5, 61.5, and 51.5 nm for MOF-808, Ex-MOF-808(NH_2), Ex-MOF-808(NO_2), Ex-MOF-808(H), Mix-MOF-808(NH_2), Mix-MOF-808(NO_2) and Mix-MOF-808(H), respectively.

Table 2
Zeta potential of MOF-808-based catalysts.

Structure	Zeta potential (mV)
MOF-808	52
Ex-MOF-808(H)	2.6
Ex-MOF-808(NH_2)	15.5
Ex-MOF-808(NO_2)	0
Mix-MOF-808(H)	52.3
Mix-MOF-808(NH_2)	51.7
Mix-MOF-808(NO_2)	54.2

3.1.2. Fourier-transform infrared spectroscopy

Fourier-transform infrared (FT-IR) spectra of MOF-808, Ex-MOF-808(NH_2, NO_2, H) and Mix-MOF-808(NH_2, NO_2, H) has been illustrated in Fig. 3b. In all of the MOF-808 structures at 3432 cm^{-1}, the OH-stretching of the carboxylate group of the BTC ligand in MOF-808 has a broadening absorption peak. Also, an adsorption band at 1664 cm^{-1} existed in all graphs ascribed to the stretching vibration of C═O in DMF. At 648 cm^{-1}, the vibration peak of Zr–O is strongly observed, informing that the coordination reaction occurs between the carboxyl in groups of BTC and zirconium ion. The FT-IR spectra of MOF-808 samples exhibit the characteristic vibration peaks at 1620, 1525, and 1436 cm^{-1} due to the aromatic ring. Compared with the IR spectra of MOF-808, several new bands located at 1120 cm^{-1} and 1056 cm^{-1} appear in the IR spectra of Ex-MOF-808(NH_2, NO_2) and Mix-MOF-808(NH_2, NO_2), and these bands stem from the C–N stretching vibrations in NH_2-isoBDC and NO_2-isoBDC ligands. Besides, the N–H stretching vibration band in the IR spectra of Ex-MOF-808(NH_2) and Mix-MOF-808(NH_2), at 3125 cm^{-1}, but is not observed due to the presence of large amounts of hydroxyl groups in the spectra.

3.1.3. Thermal gravimetric analysis

To further confirm the stability rate of the modified Ex-MOF-808(NH_2, NO_2, H) and mix-MOF-808(NH_2, NO_2, H) samples compared to MOF-808, thermal gravimetric analysis was performed under argon condition, as demonstrated in Fig. 3c. According to the diagram, the prepared mix-MOF-808(NH_2, NO_2, H) samples have a similar profile to MOF-808 and the destruction of the frameworks happens gradually in the range of 250–600 °C. In this case, the homogenous spreading of the second linker in mixed-linker MOFs causes it to demonstrate similar thermal behavior to MOF-808. On the contrary, the Ex-MOF-808(NH_2, NO_2, H) dehydroxylation of the zirconium oxo-clusters occurs in a smaller temperature range of about 450–600 °C. Generally, a tangible difference can be observed in the TGA diagram of the Zr-MOF networks and all frameworks are stable up to 600 °C.

3.1.4. N_2 sorption

Nitrogen sorption isotherms of MOF-808, Ex-MOF-808(NH_2, NO_2, H), and Mix-MOF-808(NH_2, NO_2, H) were measured at 77 K (Fig. 3d). Formerly, all the prepared compounds were activated at 110 °C for 12 h under a vacuum. According to Fig. 3d, it can be seen that the isotherms of all catalysts show a type-IV curve, which indicates that the samples obtained from mixing and exchanged-ligand methods have a mesoporous nature. Table 1 illustrates a summary of the textural properties of MOF-808 and its derivatives. According to Tables 1 it can be seen that the surface area and pore volume of MOF-808 decrease after loading secondary ligands, which shows that the secondary ligands are well placed inside the MOF-808 and the pores are more limited, and as a result, the surface area is reduced. For instance, Ex-MOF-808-NH_2 functionalized by amino groups ultimately has less porosity than the parent MOF-808 due to the filling of confined spaces by NH_2 groups [39]. In other words, the surface area and pore volume of samples systematically decrease by incorporation of NH_2-isoBDC ligand within the framework.

3.1.5. Scanning electron microscopy

Scanning electron microscopy images were used to confirm the morphology and particle size of the MOFs. The bare MOF-808 has a spherical morphology and this shape remains in mix-MOF-808(H) (Fig. 4a and b). As presented in Fig. 4c and d, the average particle size for MOF-808 and mix-MOF-808(H) was calculated 116.04, and 92.2 nm, respectively.

3.1.6. Zeta potential

To investigate the charge state of MOF-808, Ex-MOF-808(NH_2), Ex-MOF-808(NO_2), Ex-MOF-808(H), Mix-MOF-808(NH_2), Mix-MOF-808(NO_2) and Mix-MOF-808(H) structures, the zeta potential method was carried out (Table 2). From the zeta potential measurement, it was found that the surface charge of MOF-808 at neutral pH was 52 mV. A similar positive charge was observed in mix-linker constructed samples (Mix-MOF-808(NH_2, NO_2, H)). Regarding samples obtained from the exchanged-ligand method, the surface charge is more negative than the mixing-ligand method. This analysis shows that in the exchange method, the highest exchange rate is done at the surface of the nanoparticles, and as a result, the amount of defect and functional groups is higher at the surface, which also affects the catalytic activity [40,41].

3.2. Performance in oxidation of methyl phenyl sulfide

The oxidative desulfurization of organic sulfides is becoming the most viable method for eliminating stubborn naturally occurring sulfides from fossil fuels, so researchers are continuing to develop high-efficiency solid catalysts for sulfide oxidation [42,43]. In our

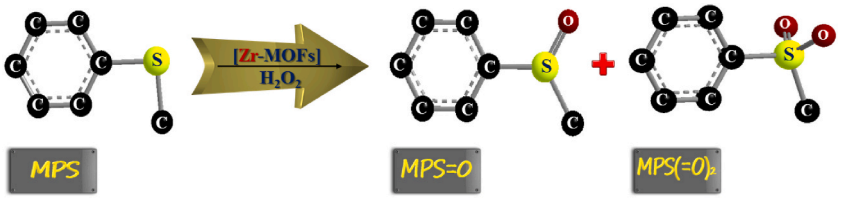

Fig. 5. Oxidation of methyl phenyl sulfide (MPS) with H_2O_2 over Zr-MOFs.

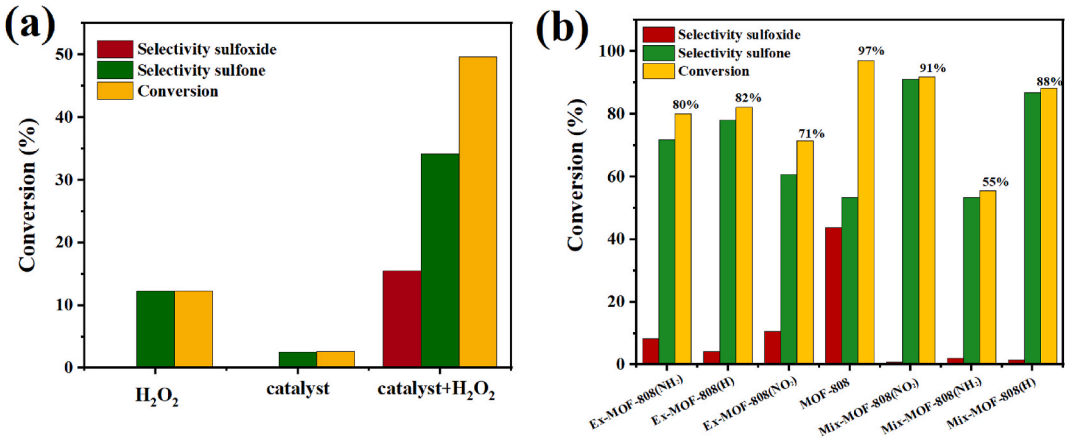

Fig. 6. (a) Effect of [H_2O_2]/[thioanisole] ratio is 1:1 on sulfoxidation conversion at 25 °C in acetonitrile solvent, Ex-MOF-808(NH_2) catalyst (0.01 mmol), reaction time = 15 min, (b) Effect of reaction of different catalysts on oxidation of thioanisole (0.1 mmol) with H_2O_2 (0.2 mmol) in acetonitrile solvent, catalyst (0.01 mmol), reaction time = 5 min.

Table 3
Experimental Data conversion of MPS using various materials as the catalyst.

Catalyst type	Conversion (%)
MOF-808	97
Ex-MOF-808(NH_2)	80
Ex-MOF-808(NO_2)	71
Ex-MOF-808(H)	82
Mix-MOF-808(NH_2)	55
Mix-MOF-808(NO_2)	91
Mix-MOF-808(H)	88

Experimental condition: thioanisol (0.1 mmol) with H_2O_2 (0.2 mmol) in acetonitrile solvent, catalyst (0.01 mmol), reaction time = 5 min.

project, a well-known methyl phenyl sulfide (MPS) was utilized as a model reaction for sulfide oxidation. The sulfur atom of the methyl phenyl sulfide is electron-rich and has been shown to undergo electrophilic oxidation to give sulfoxide [44]. The oxidation process was performed with hydrogen peroxide as an oxidant, which can oxidize thioanisole compounds and convert them into the corresponding sulfoxide or sulfone products. Meanwhile, CH_3CN is used as a solvent for the oxidation process to drag the polar sulfoxide and sulfone products out of the pores in the catalysts and make more active catalytic sites. The concentration of MPS was monitored by analyzing reaction products at intervals on a GC-MS. The overall reaction schematic is illustrated in Fig. 5.

Interestingly, the use of defect-engineered MOFs, Ex-MOF-808(NH_2, NO_2, H) and Mix-MOF-808 (NH_2, NO_2, H), containing defect-inducing linkers, led to the creation of functional groups and open metal sites in frameworks which can modify the catalytic performance [45]. Also, different strategies have been used to introduce multiple functional ligands such as mixed-ligand MOFs and ligand-exchanged MOFs. Most commonly, mixed-ligand MOFs have been prepared by solvothermal synthesis from ligand mixtures [46]. In this study, Mix-MOF-808(NH_2), Mix-MOF-808(NO_2), and Mix-MOF-808(H) were gained from the mixed-ligand strategy. In this method, homogenous dispersion of the second linker was observed in the final structures which were confirmed by zeta potential analysis. In the following, many catalytic tests were investigated in different conditions to identify better the effect of each of the created functional groups.

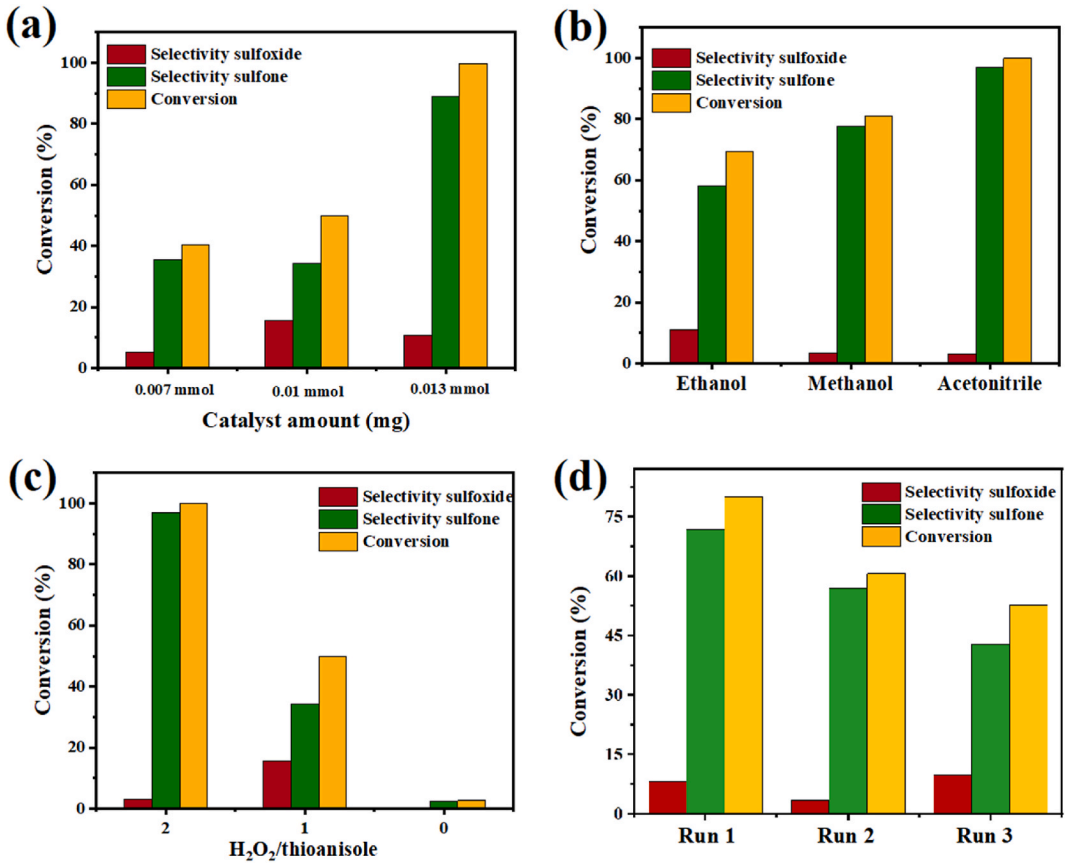

Fig. 7. Optimization of oxidation reaction parameters (a) effect of catalyst dosage, (d) influence of solvent, (c) different amount of oxidant (Reaction condition: sulfide (0.1 mmol), T = 25 °C, reaction time = 15 min), and (d) Reused experiments for Ex-MOF-808(NH_2) the oxidation of MPS under optimal conditions.

As a first catalytic test, Ex-MOF-808(NH_2) was chosen randomly as a catalyst to investigate the effect of the presence of H_2O_2 and catalyst in the MPS reaction. The catalytic reaction was performed under [H_2O_2]/[thioanisole] ratio 1:1 at 25 °C in acetonitrile solvent condition. It was indicated that the presence of an oxidant agent was necessary for the accomplishment of the reaction. Then the reaction occurred in the lack of a catalyst, and the results show that no oxidation occurred in the lack of the catalyst (Fig. 6a).

After enormous catalytic tests, the reaction condition was optimized. The oxidation of MPS (0.1 mmol) with 0.2 mmol H_2O_2 in the presence of MOF-808, Ex-MOF-808(NH_2, NO_2, H), and Mix-MOF-808(NH_2, NO_2, H) as the catalysts produced the corresponding sulfone with unprecedentedly high selectivity substrate conversion in acetonitrile solvent condition; (Fig. 6b, and Table 3). In Fig. 6b, after 5 min, the MPS oxidation rate reactivity decreased in the order of MOF-808> Mix-MOF-808(NO_2) > Mix-MOF-808(H) > Ex-MOF-808(H) > Ex-MOF-808(NH_2) > Ex-MOF-808(NO_2) > Mix-MOF-808(NH_2). Mix-MOF-808(NO_2) demonstrates the highest catalytic reactivity, for the uniform fixation of amino functions in the surface of MOF-808 as much as possible [47].

Selectivity in catalytic reactions refers to the ability of a catalyst to promote specific reactions while minimizing undesired side reactions [48]. This is crucial in various industries, including pharmaceuticals, petrochemicals, and environmental remediation. High selectivity allows for increased yield of desired products, reduces waste, and improves efficiency, ultimately leading to cost savings and environmental benefits. Achieving high selectivity often requires careful catalyst design and optimization of reaction conditions. Factors such as catalyst composition, structure, and surface properties play crucial roles in determining selectivity by influencing reaction pathways and adsorption/desorption kinetics of reactants and intermediates [49]. The importance of selectivity towards sulfone products in methyl phenyl sulfide reactions, aside from sulfoxides, lies in several key aspects:(1) Increased oxidative stability: Sulfones are generally more stable to oxidation than sulfoxides. Therefore, directing the reaction towards sulfone formation can lead to products with enhanced oxidative stability, making them more suitable for applications where exposure to air or other oxidizing agents is a concern. (2) Functional group tolerance: Sulfones can tolerate a wider range of functional groups compared to sulfoxides. By favoring sulfone formation, the reaction can proceed with higher selectivity in the presence of various functional groups, expanding the scope of compatible substrates and enabling more versatile synthetic routes. (3) Improved physicochemical properties: Sulfones often exhibit different physicochemical properties compared to sulfoxides, such as solubility, polarity, and reactivity. Selectivity towards sulfone formation can lead to products with desired properties for specific applications, such as improved solubility in organic solvents or compatibility with other materials. (4) Process efficiency: Depending on the downstream processing requirements, sulfones

Table 4
A comparison table for MPS catalytic reaction.

No.	Catalyst	Reaction time	Solvent	MPS Total Conversion	Selectivity to sulfone	Reusability	Reference
1	$P_2W_{18}Sn_3$@MIL-101	120	CH_3CN	98 %	98 %	6	[53]
2	$P_2W_{18}Ce_3$@- MIL-101	35	CH_3CN	98 %	98 %	6	[53]
3	Fe_3O_4@PEO-SO_3H	40	CH_3CN	95 %	–	–	[54]
4	Fe_3O_4@PEO-SO_3H	10	EtOH	95 %	–	8	[54]
5	UiO-67	30	CH_3CN	51 %	49 %	–	[55]
6	UiO-66 + H^+	210	CH_3CN	59 %	40 %	–	[55]
7	MIP-200	240	CH_3CN	97 %	90 %	–	[56]
8	Ex-MOF-808 (NH_2)	5	CH_3CN	80 %	72 %	3	In this work
9	Ex-MOF-808 (NH_2)	10	CH_3CN	98 %	97.7 %	–	In this work
10	Mix-MOF-808(NO_2)	5	CH_3CN	91.7 %	91.1 %	–	In this work

may offer advantages over sulfoxides in terms of ease of purification, stability during isolation, or compatibility with subsequent reactions. Selectivity towards sulfone formation can streamline the overall synthetic process and improve the efficiency of product isolation and purification steps. According to the above descriptions, although the overall efficiency of pristine MOF-808 is high, it has very low selectivity toward each product. On the other hand, other functionalized MOFs have a high selectivity toward sulfone, which is very important in catalytic applications [50,51].

NH_2-BTC in MOF-808 can serve as an effective catalyst for methyl phenyl sulfide oxidation due to the presence of the amino functional group, which can contribute to enhanced reactivity, selectivity, and stability of the catalyst in the reaction. The amino group can act as a Lewis base, facilitating the activation of the oxidant and the substrate. The presence of the amino group can stabilize reaction intermediates through hydrogen bonding or other interactions, which may lower the activation energy of the reaction steps involved in the oxidation of methyl phenyl sulfide.

NO_2-BTC in MOF-808 may exhibit different catalytic behavior compared to NH_2-BTC due to the distinct electronic and steric effects introduced by the nitro functional group. The electron-withdrawing nature of the NO_2 group may enhance the reactivity of the MOF catalyst, potentially leading to improved catalytic activity or selectivity in the oxidation reaction. The nitro group is strongly electron-withdrawing due to its high electronegativity. This can influence the electronic properties of the MOF and the active sites within the framework. In the context of oxidation reactions like methyl phenyl sulfide oxidation, the electron-withdrawing nature of the NO_2 group can enhance the electrophilicity of nearby metal centers, potentially facilitating the activation of the oxidant or the substrate. Also, the presence of the NO_2 group may introduce steric hindrance around the active sites of the MOF, affecting the accessibility of reactants and intermediates to the catalytic sites. This could influence the reaction kinetics and selectivity of the oxidation process.

3.2.1. Effect of different catalyst dosages on reaction

The effect of different catalyst dosages on the catalytic conversion performance for Ex-MOF-808(NH_2) was studied (Fig. 7a). After 15 min of reaction, the MPS conversion can reach 99.7 % with 0.013 mmol of Ex-MOF-808(NH_2) catalyst (reaction condition: sulfide (0.1 mmol), H_2O_2 (0.1 mmol), T = 25 °C). The results indicate that increasing the catalyst dosage enhances the conversion of MPS. Therefore, the performance has greatly improved, when the amount of catalyst is increased to 0.013 mmol, which ascribes to more opportunity for the sulfide and catalyst to contact. So, a 0.013 mmol catalyst is selected as the better dosage.

3.2.2. Effect of different solvents on reaction

In catalytic systems, the background (uncatalyzed) reaction will always take place. Many types of research show that the protic and acidic solvents have a relatively high level of background reaction, whereas the nitrile-containing aprotic solvents can suppress it [52]. The role of different solvents in the oxidation of methyl phenyl sulfide was examined in Fig. 7b. As illustrated in Fig. 7b, in the presence of Ex-MOF-808(NH_2) when we used acetonitrile as a solvent, the desired product conversion to sulfone was much better than ethanol and methanol. So, acetonitrile was chosen as a solvent, because of its documented suppression of background reaction.

3.2.3. Effect of different oxidant/sulfur ratio on reaction

As illustrated in Fig. 7c, the effect of the oxidant/sulfur (O/S) molar ratio was studied. The rise of the H_2O_2 to MPS ratio improves the performance of the catalytic reaction and shortens the time to complete sulfide oxidation (Fig. 7c). When the O/S molar ratio is 2, the conversion of MPS is 99.9 % in a reaction time of 15 min in acetonitrile solvent conditions. After comparison, an oxygen-sulfur ratio of 2 is a better choice.

3.2.4. Investigate the stability of the catalyst

One of the main advantages of heterogeneous catalysts is reusability, which is greatly important for commercial applications. To investigate the recyclability of the Ex-MOF-808(NH_2) catalyst in the MPS oxidation reaction, we designed the corresponding cycle experiments. After completing each run, the catalyst was recovered and then used for the next reaction run. The recovered sample was dried and then used directly for subsequent catalytic sulfide oxidation reactions. The results showed that the catalyst could be recycled at least 3 times with good selectivity (Fig. 7d). Subsequent PXRD analysis confirmed no significant alterations in the crystal structure following these cycles.

Table 4 illustrated a comparision between this work and previous reports of MPS reaction over MOF structures. It is worth noting

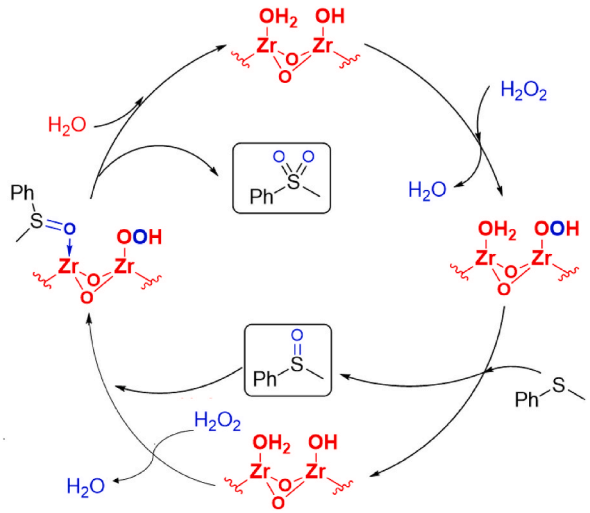

Fig. 8. Possible reaction mechanism for the oxidation of sulfides to sulfoxides over Zr-MOF-808 structures.

that the reaction time and selectivity of the synthesized catalysts is better than most of the MOFs reported in previous publications.

3.3. Possible reaction mechanism

Overall, we tentatively propose the mechanism of the oxidation of S-compounds over Zr-MOF structures. In this work, the Zr-MOF-808 catalyzed oxidation of methyl phenyl sulfide, particularly in the presence of hydrogen peroxide (H_2O_2) as the oxidant, the mechanism unfolds through a series of intricate steps. Initially, methyl phenyl sulfide adheres to the surface of Zr-MOF-808, facilitated by weak interactions. This catalyst, serving as a platform for catalytic activity, activates hydrogen peroxide, leading to the generation of reactive oxygen species like hydroperoxo or peroxo species on its surface. Subsequently, these activated oxygen species partake in the oxidation process, where one oxygen atom is transferred to the sulfur atom of the sulfide. This transfer results in the formation of two products: methyl phenyl sulfoxide and methyl phenyl sulfone. Methyl phenyl sulfoxide is formed when the oxygen atom attaches to the sulfur atom with a single bond, while methyl phenyl sulfone is produced when the oxygen atom attaches to the sulfur atom with a double bond. Following the completion of the oxidation step, both the sulfoxide and sulfone products desorb from the catalyst surface, leaving behind a regenerated Zr-MOF-808 catalyst (Fig. 8). Overall, the mechanism underscores the pivotal role of Zr-MOF-808 in mediating the oxidation of methyl phenyl sulfide, especially in the presence of hydrogen peroxide, offering insights into its catalytic prowess in organic transformations [28,55].

4. Conclusion

In the present study, a series of functionalized and de-functionalized Zr-MOF-808 structures were successfully fabricated with two different synthesis strategies; the mixed linker method and the post-synthesis linker exchange method. In this study, Mix-MOF-808 (NH_2), Mix-MOF-808(NO_2), and Mix-MOF-808(H) were gained from the mixed-ligand strategy have uniform dispersion of linkers in hole framework and the surface charge of catalyst is more similar to pristine MOF-808. Also, Ex-MOF-808(NH_2), Ex-MOF-808(NO_2), and Ex-MOF-808(H) which synthesize by ultrasound-assisted exchange method have a more negative surface charge. All the synthesized catalysts were compared in the MPS oxidation reaction. According to the results Mix-MOF-808(NO_2) demonstrates 91 % conversion with high selectivity toward sulfone product. Also, all functional MOFs have a high selectivity to sulfone which cannot illustrated in pristine MOF-808. It should be noted that the selectivity of a catalyst refers to the ability of a catalyst to promote specific reactions while minimizing undesired side reactions which was crucial in industrial applications.

Data availability statement

Data will be made available on request. Further information and requests for resources should be directed to the lead contact, Vahid Safarifard (vsafarifard@iust.ac.ir).

CRediT authorship contribution statement

Negin Khosroshahi: Writing – original draft, Project administration, Conceptualization. **Samira Doaee:** Writing – original draft, Formal analysis, Conceptualization. **Vahid Safarifard:** Writing – review & editing, Supervision. **Sadegh Rostamnia:** Writing – review & editing, Supervision.

Declaration of competing interest

The authors declare that they have no known competing financial interests or personal relationships that could have appeared to influence the work reported in this paper.

Acknowledgments

Support for this investigation by the Iran University of Science and Technology is gratefully acknowledged.

Appendix A. Supplementary data

Supplementary data to this article can be found online at https://doi.org/10.1016/j.heliyon.2024.e31254.

References

[1] M.D. Goudarzi, N. Khosroshahi, V. Safarifard, Exploring novel heterojunctions based on the cerium metal–organic framework family and CAU-1, as dissimilar structures, for the sake of photocatalytic activity enhancement, RSC Adv. 12 (50) (2022) 32237–32248.
[2] M. Hosseinpour, N. Khosroshahi, V. Safarifard, Construction of a Ce-UiO-66/MCo2O4 heterojunction for photocatalytic Cr (VI) detoxification through "p-n junction" mechanism, ChemPhotoChem 7 (9) (2023) e202200323.
[3] L. Chen, R. Luque, Y. Li, Controllable design of tunable nanostructures inside metal–organic frameworks, Chem. Soc. Rev. 46 (15) (2017) 4614–4630.
[4] A.H. Valekar, et al., Catalytic transfer hydrogenation of furfural to furfuryl alcohol under mild conditions over Zr-MOFs: exploring the role of metal node coordination and modification, ACS Catal. 10 (6) (2020) 3720–3732.
[5] M. Bakhtian, N. Khosroshahi, V. Safarifard, Efficient removal of inorganic and organic pollutants over a NiCo2O4@ MOF-801@ MIL88A photocatalyst: the significance of ternary heterojunction engineering, ACS Omega 7 (47) (2022) 42901–42915.
[6] L. Chen, Q. Xu, Metal-organic framework composites for catalysis, Matter 1 (1) (2019) 57–89.
[7] H.-Q. Zheng, et al., Zr-based metal–organic frameworks with intrinsic peroxidase-like activity for ultradeep oxidative desulfurization: mechanism of H2O2 decomposition, Inorg. Chem. 58 (10) (2019) 6983–6992.
[8] S. Rong, et al., Postsynthetic modification of metal–organic frameworks by vapor-phase grafting, Inorg. Chem. 60 (16) (2021) 11745–11749.
[9] C. Ardila-Suárez, et al., Enhanced acidity of defective MOF-808: effects of the activation process and missing linker defects, Catal. Sci. Technol. 8 (3) (2018) 847–857.
[10] H.-H. Mautschke, et al., Catalytic properties of pristine and defect-engineered Zr-MOF-808 metal organic frameworks, Catal. Sci. Technol. 8 (14) (2018) 3610–3616.
[11] J. Hajek, et al., Mechanistic studies of aldol condensations in UiO-66 and UiO-66-NH2 metal organic frameworks, J. Catal. 331 (2015) 1–12.
[12] M. Sadakiyo, Support effects of metal–organic frameworks in heterogeneous catalysis, Nanoscale 14 (9) (2022) 3398–3406.
[13] L. Zhang, et al., Rational design of smart adsorbent equipped with a sensitive indicator via ligand exchange: a hierarchical porous mixed-ligand MOF for simultaneous removal and detection of Hg2+, Nano Res. 14 (5) (2021) 1523–1532.
[14] C. Xu, et al., Functional metal–organic frameworks for catalytic applications, Coord. Chem. Rev. 388 (2019) 268–292.
[15] Y. Qin, et al., Post-synthetic modifications (PSM) on metal–organic frameworks (MOFs) for visible-light-initiated photocatalysis, Dalton Trans. 50 (38) (2021) 13201–13215.
[16] M. Taddei, et al., Post-synthetic ligand exchange in zirconium-based metal–organic frameworks: beware of the defects, Angew. Chem. Int. Ed. 57 (36) (2018) 11706–11710.
[17] S.M. Cohen, Postsynthetic methods for the functionalization of metal–organic frameworks, Chem. Rev. 112 (2) (2012) 970–1000.
[18] Z. Yin, et al., Recent advances in post-synthetic modification of metal–organic frameworks: new types and tandem reactions, Coord. Chem. Rev. 378 (2019) 500–512.
[19] O. Karagiaridi, et al., Solvent-assisted linker exchange: an alternative to the de novo synthesis of unattainable metal–organic frameworks, Angew. Chem. Int. Ed. 53 (18) (2014) 4530–4540.
[20] O. Karagiaridi, et al., Functionalized defects through solvent-assisted linker exchange: synthesis, characterization, and partial postsynthesis elaboration of a metal–organic framework containing free carboxylic acid moieties, Inorg. Chem. 54 (4) (2015) 1785–1790.
[21] J.-S. Qin, et al., Mixed-linker strategy for the construction of multifunctional metal–organic frameworks, J. Mater. Chem. A 5 (9) (2017) 4280–4291.
[22] Y. Fu, et al., Enabling simultaneous redox transformation of toxic chromium (VI) and arsenic (III) in aqueous media—a review, J. Hazard Mater. 417 (2021) 126041.
[23] Z. Qi, et al., Synthesis of ionic-liquid-functionalized UiO-66 framework by post-synthetic ligand exchange for the ultra-deep desulfurization, Fuel 268 (2020) 117336.
[24] A.G. Moaser, et al., Curbed of molybdenum oxido-diperoxido complex on ionic liquid body of mesoporous Bipy-PMO-IL as a promising catalyst for selective sulfide oxidation, J. Mol. Liq. 312 (2020) 113388.
[25] E. Doustkhah, et al., Merging periodic mesoporous organosilica (PMO) with mesoporous aluminosilica (Al/Si-PMO): a catalyst for green oxidation, Mol. Catal. 482 (2020) 110676.
[26] S. Rostamnia, et al., NH2-coordinately immobilized tris (8-quinolinolato) iron onto the silica coated magnetite nanoparticle: Fe3O4@ SiO2-FeQ3 as a selective Fenton-like catalyst for clean oxidation of sulfides, J. Colloid Interface Sci. 511 (2018) 447–455.
[27] J. Drabowicz, M. Mikołajczyk, An improved method for oxidation of sulfides to sulfoxides with hydrogen peroxide in methanol, Synth. Commun. 11 (12) (1981) 1025–1030.
[28] I. Martausová, et al., Catalytic activity of advanced titanosilicate zeolites in hydrogen peroxide S-oxidation of methyl (phenyl) sulfide, Catal. Today 324 (2019) 144–153.
[29] K. Tanaka, et al., Asymmetric catalytic sulfoxidation with H2O2 using chiral copper metal–organic framework crystals, Asian Journal of Organic Chemistry 2 (12) (2013) 1055–1060.
[30] E. Skolia, P.L. Gkizis, C.G. Kokotos, Aerobic photocatalysis: oxidation of sulfides to sulfoxides, ChemPlusChem 87 (4) (2022) e202200008.
[31] J. Li, et al., Heteropolyacid supported MOF fibers for oxidative desulfurization of fuel, Chem. Eng. J. 388 (2020) 124325.
[32] S. Zhou, et al., Metal-organic framework encapsulated high-loaded phosphomolybdic acid: a highly stable catalyst for oxidative desulfurization of 4, 6-dimethyldibenzothiophene, Fuel 309 (2022) 122143.
[33] C. Wang, et al., Preparation of formate-free PMA@ MOF-808 catalysts for deep oxidative desulfurization of model fuels, Environ. Sci. Pollut. Control Ser. 29 (26) (2022) 39427–39440.
[34] O. Kholdeeva, N. Maksimchuk, Metal-organic frameworks in oxidation catalysis with hydrogen peroxide, Catalysts 11 (2) (2021) 283.

[35] F.E. Chen, et al., A structure–activity study of aromatic acid modulators for the synthesis of zirconium-based metal–organic frameworks, Chem. Mater. 34 (7) (2022) 3383–3394.
[36] N. Khosroshahi, M. Bakhtian, V. Safarifard, Mechanochemical synthesis of ferrite/MOF nanocomposite: efficient photocatalyst for the removal of meropenem and hexavalent chromium from water, J. Photochem. Photobiol. Chem. 431 (2022) 114033.
[37] L. Chu, et al., Excellent catalytic performance over acid-treated MOF-808 (Ce) for oxidative desulfurization of dibenzothiophene, Fuel 332 (2023) 126012.
[38] K.E. Hicks, et al., The dependence of olefin hydrogenation and isomerization rates on zirconium metal–organic framework structure, ACS Catal. 12 (21) (2022) 13671–13680.
[39] Y. Horiuchi, et al., Visible-light-promoted photocatalytic hydrogen production by using an amino-functionalized Ti (IV) metal–organic framework, J. Phys. Chem. C 116 (39) (2012) 20848–20853.
[40] C. Ji, et al., High-efficiency and sustainable desalination using thermo-regenerable MOF-808-EDTA: temperature-regulated proton transfer, ACS Appl. Mater. Interfaces 13 (20) (2021) 23833–23842.
[41] M. Karimi, et al., Confined-based catalyst investigation through the comparative functionalization and defunctionalization of Zr-MOF, RSC Adv. 12 (26) (2022) 16358–16368.
[42] C.G. Piscopo, et al., Metal-organic framework-based catalysts for oxidative desulfurization, ChemCatChem 12 (19) (2020) 4721–4731.
[43] X.-N. Zou, et al., Incorporating photochromic triphenylamine into a zirconium–organic framework for highly effective photocatalytic aerobic oxidation of sulfides, ACS Appl. Mater. Interfaces 13 (17) (2021) 20137–20144.
[44] M.R. Maurya, A.K. Chandrakar, S. Chand, Zeolite-Y encapsulated metal complexes of oxovanadium (VI), copper (II) and nickel (II) as catalyst for the oxidation of styrene, cyclohexane and methyl phenyl sulfide, J. Mol. Catal. Chem. 274 (1–2) (2007) 192–201.
[45] X. Feng, et al., Generating catalytic sites in UiO-66 through defect engineering, ACS Appl. Mater. Interfaces 13 (51) (2021) 60715–60735.
[46] J. Canivet, M. Vandichel, D. Farrusseng, Origin of highly active metal–organic framework catalysts: defects? Defects, Dalton Trans. 45 (10) (2016) 4090–4099.
[47] F. Vermoortele, et al., An amino-modified Zr-terephthalate metal–organic framework as an acid–base catalyst for cross-aldol condensation, Chem. Commun. 47 (5) (2011) 1521–1523.
[48] S. Doherty, et al., Efficient and selective hydrogen peroxide-mediated oxidation of sulfides in batch and segmented and continuous flow using a peroxometalate-based polymer immobilised ionic liquid phase catalyst, Green Chem. 17 (3) (2015) 1559–1571.
[49] W. Al-Maksoud, S. Daniele, A.B. Sorokin, Practical oxidation of sulfides to sulfones by H 2 O 2 catalysed by titanium catalyst, Green Chem. 10 (4) (2008) 447–451.
[50] G.A. Somorjai, J.Y. Park, Molecular factors of catalytic selectivity, Angew. Chem. Int. Ed. 47 (48) (2008) 9212–9228.
[51] K. An, G.A. Somorjai, Size and shape control of metal nanoparticles for reaction selectivity in catalysis, ChemCatChem 4 (10) (2012) 1512–1524.
[52] R. Cibulka, Artificial flavin systems for chemoselective and stereoselective oxidations, Eur. J. Org Chem. 2015 (5) (2015) 915–932.
[53] E. Naseri, R. Khoshnavazi, Sandwich type polyoxometalates encapsulated into the mesoporous material: synthesis, characterization and catalytic application in the selective oxidation of sulfides, RSC Adv. 8 (49) (2018) 28249–28260.
[54] J. Rahimi, et al., An efficient superparamagnetic PEO-based nanocatalyst for selective oxidation of sulfides to sulfoxides, Inorg. Chem. Commun. 148 (2023) 110320.
[55] O.V. Zalomaeva, et al., Nucleophilic versus electrophilic activation of hydrogen peroxide over Zr-based metal–organic frameworks, Inorg. Chem. 59 (15) (2020) 10634–10649.
[56] N.V. Maksimchuk, et al., Catalytic performance of Zr-based metal–organic frameworks Zr-abtc and MIP-200 in selective oxidations with H2O2, Chem.–Eur. J. 27 (23) (2021) 6985–6992.